^{23}Na-NMR study on the one-dimensional superoxide spin-chain compound NaO_2

Takayuki Goto*
Physics Division, Faculty of Science and Technology, Sophia University, Chiyodaku 102-8554, Japan

Mizuki Miyajima and Takashi Kambe
Department of Physics, Okayama University, Okayama 700-8530, Japan

(Received 15 October 2025; revised 4 September 2026; accepted 5 October 2026; published 2 November 2026)

We report a ^{23}Na-NMR study of the alkali superoxide NaO_2, a candidate one-dimensional quantum spin system. The Knight shift, linewidth, and spin-lattice relaxation rate $1/T_1$ were investigated down to 0.3 K in magnetic fields up to 16 T. Below $T_{S3} = 34$ K, $1/T_1$ exhibits thermally activated behavior, indicating the opening of a spin gap of $\Delta(10.1\ \mathrm{T}) \simeq 38.0$ K and $\Delta(3.55\ \mathrm{T}) \simeq 46$ K. The hyperfine coupling constant shows a sudden reduction across the structural transition at $T_{S2} \simeq 195$ K, reflecting the development of pronounced one-dimensionality in the electron structure. These results provide microscopic evidence that NaO_2 is a rare π-orbital-based one-dimensional spin chain that exhibits a spin-gapped ground state, consistent with a spin-Peierls-like instability.

DOI: 10.1103/8bvh-ld52

I. INTRODUCTION

Low-dimensional quantum spin systems have recently attracted considerable interest. Quantum fluctuations, together with reduced dimensionality, suppress long-range magnetic order and enhance the possibility of exotic quantum phases, such as spin liquids [1–4]. In this paper, we investigate the alkali superoxide NaO_2, a candidate one-dimensional quantum spin system. A previous study by Miyajima *et al.* has shown that the compound undergoes a three-step structural phase transformation from phase I to phase IV. Upon cooling from room temperature, the system exhibits a structural phase transition at $T_{S1} = 240$ K from phase I (space group $Fm\bar{3}m$) to phase II ($Pa\bar{3}$), and at $T_{S2} \simeq 195$ K to phase III ($Pnnm$) with an orthorhombic structure, and finally at $T_{S3} = 34$ K to phase IV, for which the space group has not been clarified yet. In phase IV, the drastic reduction in the magnetic susceptibility χ was observed, indicating the energy gap $\Delta = 51.2$ K in the spin excitation spectrum [5]. The existence of the gap is also confirmed by inelastic neutron scattering and muon spin relaxation (μSR) experiments.

Unlike the other alkali-metal superoxides, such as KO_2 [6,7], RbO_2 [8], and CsO_2 [9–12], this system does not show any long-range magnetic order down to 0.3 K, as proved by μSR measurements [5]. By the detailed x-ray diffraction (XRD) analysis on the atomic position in phase III, they have revealed that "O_2^- dumbbells" are aligned along the c axis, making good one-dimensionality in this system. Although this strongly indicates that the gap originates from the spin-Peierls transition [13–15], no direct evidence of atomic dimerization was found so far. In this paper, ^{23}Na NMR measurements provide microscopic insight into the ground state of this compound and the one-dimensional nature of the magnetic interactions.

II. EXPERIMENT

The powder sample of NaO_2 was prepared by the mixed solution method using liquid ammonia NH_3 and methyl amine CH_3NH_2 as described in Ref. [5]. A sample of approximately 0.1 g was sealed in an airtight Teflon cell in Ar atmosphere in a glove box. ^{23}Na-NMR was measured in applied magnetic fields between 3 and 16 T over the temperature range between 0.3 and 250 K. The spectra were obtained by plotting the amplitude of spin echo against applied field, which was slowly ramped up [16,17]. Figure 1 shows the entire profile of the spectrum measured at 90 K (phase III). One can clearly see the singular points corresponding to the satellite transitions ($I_Z = \pm 1/2 \leftrightarrow \pm 3/2$), 90° peaks breaking apart due to the appreciably large value of η, which is proportional to the local orthorhombicity, and 0° edges [16,17]. These observations confirm the high quality of the sample.

The nuclear spin-lattice relaxation rate $1/T_1$ was determined by the repetition method, in which the nuclear spin magnetization was traced as changing the measurement interval τ, until the difference from the thermal equilibrium value became less than 1% [18]. Figure 2 shows typical recovery curves [19,20] obtained at several temperatures. Recovery curves were analyzed by the standard formula $1 - 0.9e^{-6\tau/T_1} - 0.1e^{-\tau/T_1}$ for the central transition of nuclear spin levels $I_z = \pm 1/2$ [21].

The distance between nearest-neighboring Na and O is 2.424 Å in phase III, and 2.421 Å in phase II. These short distances indicate that ^{23}Na-NMR is expected to probe the magnetism of $S = 1/2$ spin in the O_2^- molecule. We will discuss the hyperfine coupling later.

*Contact author: gotoo-t@sophia.ac.jp

Published by the American Physical Society under the terms of the Creative Commons Attribution 4.0 International license. Further distribution of this work must maintain attribution to the author(s) and the published article's title, journal citation, and DOI.

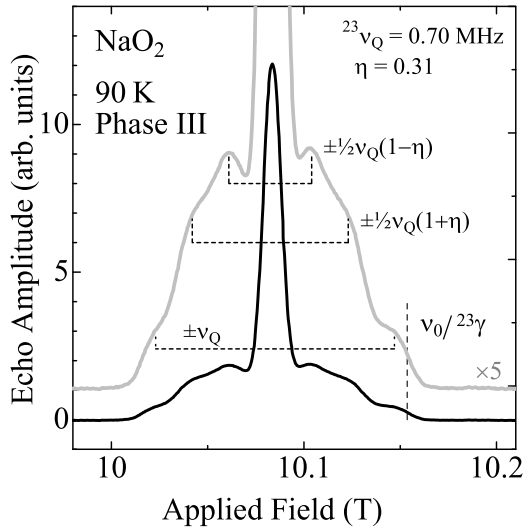


FIG. 1. Typical ^{23}Na-NMR spectra of a powder sample measured at 90 K (phase III). The dashed vertical line shows the zero-shift position $\nu_0/^{23}\gamma$, where ν_0 is the resonance frequency, and $^{23}\gamma = 11.262$ MHz/T the nuclear gyromagnetic ratio for ^{23}Na. The enlarged spectrum (gray curve) highlights the singular points associated with the quadrupole splitting of the $I = 3/2$ nucleus, shown by dotted lines. From the spacing of these features, the quadrupole frequency $^{23}\nu Q = 0.7$ MHz and the asymmetry parameter $\eta = 0.31$ were obtained.

III. RESULTS

Figure 3 shows powder patterns of entire spectra at various temperatures between 90 and 2.6 K in phases III and IV. While the position of the center peak scarcely moves, the linewidth shows a pronounced increase as the temperature is lowered.

The temperature dependence of the Knight shift and the linewidth is shown in Fig. 4. First, the Knight shift, that is, the local susceptibility at the Na site, exhibits only a weak temperature dependence. With decreasing temperature from 250 K, where the system resides in phase I, the shift shows a slight increase in proportion to the uniform susceptibility χ, but keeps nearly constant within phase III. Below T_{S3}, where

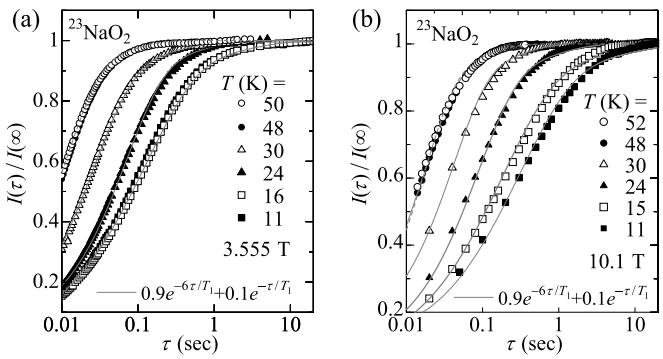


FIG. 2. Representative recovery curves of the nuclear spin magnetization [19,20] under the two magnetic fields (a) 3.554 T and (b) 10.1 T. The spin-lattice relaxation time T_1 is determined by fitting to the standard relaxation function for the central transition for $I = 3/2$ spins (solid curves) [21].

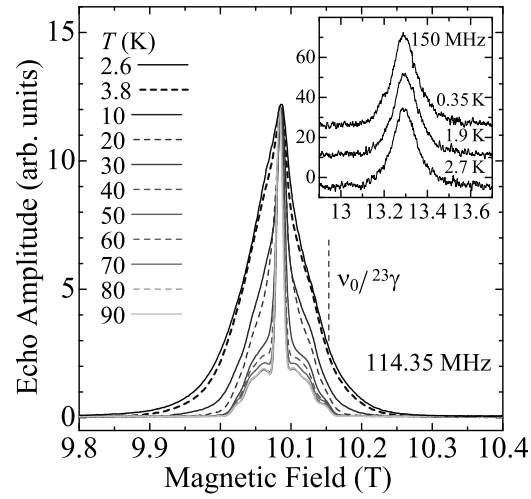


FIG. 3. Powder ^{23}Na-NMR spectra measured at several temperatures in phases III and IV. The dashed vertical line marks the zero-shift position of the ^{23}Na nucleus. The inset shows the spectra obtained at low temperatures down to 0.3 K, utilizing a ^{3}He cryostat.

χ exhibits a drastic reduction to zero, the shift follows it and slightly decreases. Proportionality between the two is shown as the K-χ plot (Fig. 5), where one can see that the isotropic hyperfine coupling constant A defined as $K = A\chi + \text{const}$, exhibits an abrupt decrease at T_{S2} from 0.61(5) T/μ_B in phases I and II to 0.07(1) T/μ_B in phase III [22]. This abrupt decrease in A is due to the fact that the transition from phase II ($Pa\bar{3}$) to phase III ($Pnnm$) is a first-order structural phase transition, which is confirmed by χ (Fig. 4) and by the NMR spectral profile (Fig. 6), both of which exhibit hysteresis in the ther-

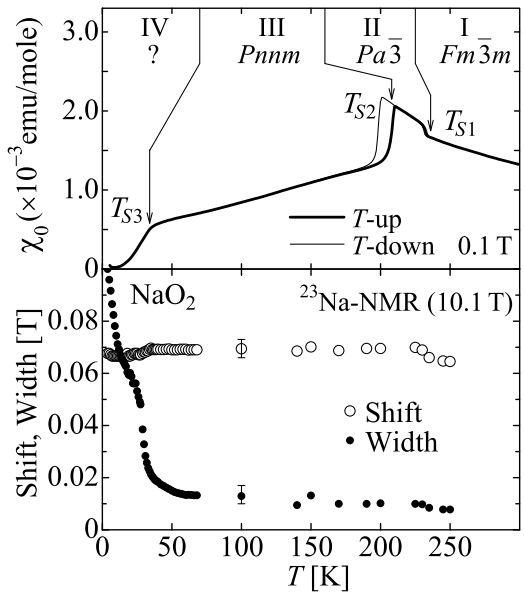


FIG. 4. Top: Temperature dependence of the magnetic susceptibility, with the low-temperature Curie term, corresponding to 1.5% of free spin in moles, subtracted [5]. Arrows indicate the structural transition temperatures T_{S1}, T_{S2}, and T_{S3}. Bottom: Temperature dependence of the Knight shift and the linewidth (FWHM) of the ^{23}Na-NMR spectrum at 10.1 T.

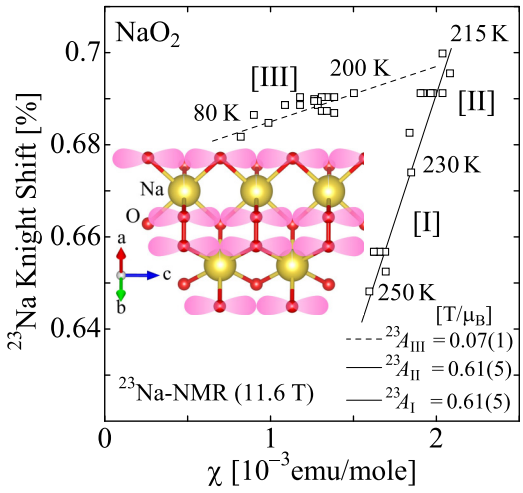


FIG. 5. Knight shift vs uniform susceptibility (K-χ plot) in phases I–III. In each phase, the data exhibit a linear relationship, from which the isotropic hyperfine coupling constant A was extracted: $A_{\rm I} = 0.61(2)$, $A_{\rm II} = 0.61(2)$, and $A_{\rm III} = 0.07(1)$ T/$\mu_{\rm B}$. The inset shows the schematic crystal structure in phase III, where the O_2 molecules are aligned along the c axis (see text).

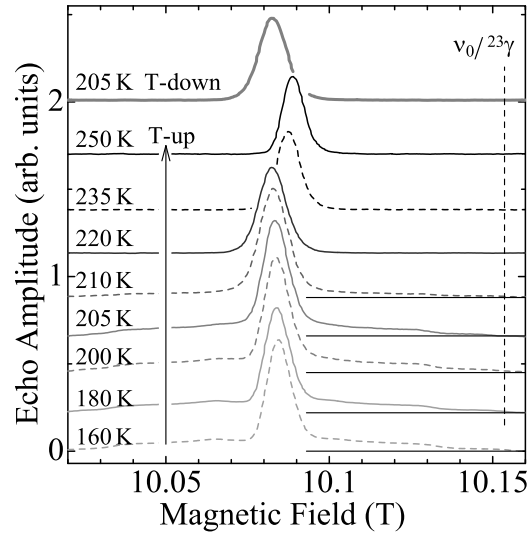


FIG. 6. ^{23}Na NMR spectra measured in phases I–III. In order to investigate the existence of hysteresis, the temperature was raised from 160 K (phase III, bottom) to 250 K (phase I, second from top), and then rapidly cooled to 205 K (phase III, top). The vertical solid arrow indicates the measurement sequence. The horizontal baselines under each spectrum emphasize the spectral tails observed below 210 K. The disappearance of the eqQ-derived spectral tails at 220 K signals the transition from the orthorhombic phase III to the cubic phase II across T_{S2}. The top spectrum at 205 K shows a tailless profile, which is a characteristic of phase I/II. Note the existence of significant eqQ tails in the 205-K data measured during the heating process. This difference clearly demonstrates the existence of hysteresis, and hence the first-order structural phase transition.

mal cycle. This finding directly reflects the one-dimensional character in phase III, as discussed below.

Below T_{S3}, both K and χ exhibit a distinct decrease. Especially the latter goes to zero with lowering temperature. In phase IV, there is a significant nonlinearity between M and the applied field [5], indicating that the comparison of χ and the NMR shift measured under different magnetic fields loses its meaning. We therefore did not try to perform the K-χ plot in this region. However, we can safely say at least that the observed decrease in K must reflect that in χ.

Next, we proceed to the temperature dependence of the linewidth, which monotonically increases from 250 K with decreasing temperature. It abruptly starts to increase at around the border between phases III and IV, exhibiting a kind of shoulder at around 20 K, and steeply increases again down to 2.6 K, where the full width at half maximum (FWHM) reaches 0.1 T. At still lower temperature, it saturates down to 0.35 K.

The spectral profile shown in Fig. 3 indicates that the prominent broadening below 40 K (4) is of a magnetic origin rather than of the electric quadrupole-quadrupole (eqQ) interaction, That is to say, if the latter was the dominant contribution to the linewidth, significant broadening should appear only in the tail part but also in the central peak [23], because it contributes to the linewidth of the center peak and satellite tails through the second and first perturbation, respectively. In fact, both the central peak and tails are broadened equally below 40 K, indicating that the magnetic inhomogeneity is evidently dominant. Furthermore, one can immediately conclude that its origin is due to some impurity part rather than the intrinsic part of the NaO_2 sample. This is because the observed temperature dependence of the linewidth does not trace that of χ, below 40 K, where the linewidth starts steeply increasing while χ goes down to zero. The short distance between the Na nucleus and the O_2^- ion stated above must bring a rather large contribution to the linewidth through the anisotropic part of the hyperfine interaction, including the classical dipole-dipole interaction; here, note that it does not contribute to the Knight shift. The observed apparent discrepancy between χ and the linewidth below T_{S3} immediately leads to the conclusion that the linewidth is contributed from the extrinsic part of the sample, that is, from impurities, which in fact are observed as the Curie term in χ [5]. The existence of this huge broadening prevented us from investigating a change in the eqQ interaction below T_{S3}. It might give information about unfound structural changes such as dimering [4,13,14,24].

Next, we move on to the behavior of $1/T_1$ shown in Fig. 7. On cooling from 60 K in phase III, $1/T_1$ starts to decrease at 45 K and shows the linear dependence against temperature. This dependence was observed commonly for the two different magnetic fields 3.554 and 10.1 T, although the magnitude of $1/T_1$ was quite different. This sensitivity to the applied field reflects the one-dimensional (1D) nature of spin systems, where $1/T_1$ is dominated by the steep valley of dispersion at $q = \pi$, the position of which moves with the applied field, influencing $1/T_1$ [25,26].

At T_{S3}, $1/T_1$ declines precipitously and exhibits a thermal-activation-type temperature dependence. However, this tendency ceases at around 20 K, below which $1/T_1$ forms a small hump at 12 and 15 K for 3.554 and 10.1 T, respectively, and decreases again gradually down to 2.5 K. The height of the hump also depends on the applied magnetic field; it seems to be suppressed under higher fields.

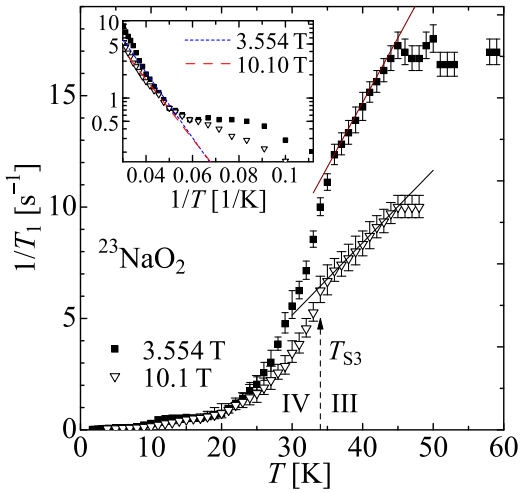


FIG. 7. Temperature dependence of the spin-lattice relaxation rate $1/T_1$ under the magnetic fields 3.554 and 10.1 T. The vertical dashed arrow marks the transition temperature T_{S3}, the boundary between phases III and IV. The solid lines indicate the linear T-temperature dependence observed between 45 K and T_{S3}. Inset: Arrhenius plot showing the thermal-activation-type temperature dependence of $1/T_1$ between T_{S3} and 20 K, below which it exhibits a humplike behavior. The dashed lines indicate the energy gaps under the magnetic field $\Delta = 38.0(2)$ K, at 10.1 T, and 46.4 K at 3.554 T.

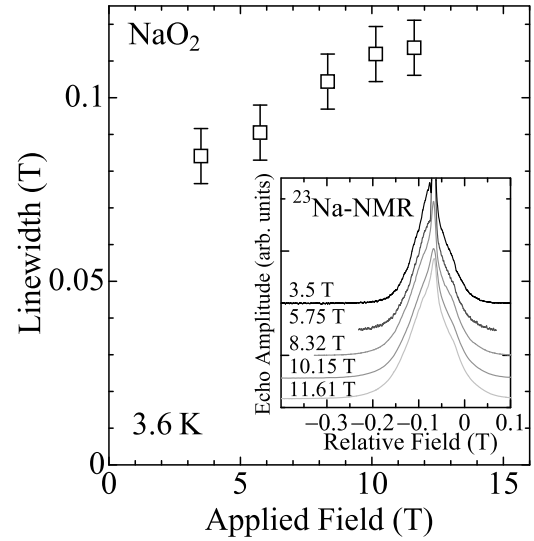


FIG. 8. Field dependence of the ^{23}Na NMR linewidth (FWHM) measured at 3.6 K. Inset: Representative spectra measured under various applied fields.

The size of the energy gap under finite magnetic fields, shown in the inset of Fig. 7, $\Delta = 38.0(2)$ K for 3.554 T and 46.4(2) K for 10.1 T, is consistent with the zero-field gap $\Delta(0\ \mathrm{T}) = 51.2$ K obtained from χ [5]. If we consider that the first-excited state above the gap has an $S = 1$ spin, that is, the magnonlike character, where the energy level of $S_z = +1$ is lowered by Zeeman effect [18,27–29] under finite magnetic fields and shrinks the gap as $\Delta(H) = \Delta(0) - g\mu_B H$, where $g \simeq 2$ is obtained from the X-band electron spin resonance (ESR) measurement [5].

Finally, Fig. 8 shows the field dependence of a linewidth at 3.6 K, where it increases monotonically with an applied field H up to 12 T. This increase is also attributed to the impurities stated above. In the previous report, the small contribution from magnetic impurities is observed in the high-field uniform magnetization M [5].

IV. DISCUSSION

First, the existence of an energy gap in the spin excitation spectrum is clearly demonstrated by the observed thermal-activation-type temperature dependence of $1/T_1$ below T_{S3}. The slight but finite decrease in the Knight shift below T_{S3} (Fig. 4) also supports this idea and indicates that the ground state is nonmagnetic. In the previous paper [5], the possibility of spin-Peierls instability is claimed for this energy gap. The observed field dependence of the gap is consistent with this picture, that is, the excited spin state of a spin-Peierls system is characterized by the breaking of spin-singlet dimers, leading to the creation of mobile, triplet excitations known as magnons [30].

The presence of one-dimensionality is essential for the occurrence of a spin-Peierls transition. The observed extremely small isotropic part of hyperfine coupling constant within phase III, shown in Fig. 5, provides microscopic evidence for this one-dimensionality. That is, the smallness in the hyperfine-coupling constant is attributed to the lifting of the two π_g orbitals [5]. In phase III, O_2 molecules are aligned along the c axis (Fig. 5), and the lobes of the occupied π_g's with the lower energy are also directed along the axis. This realizes the one-dimensional direct exchange coupling $J/k_B = 140$ K [5], and at the same time reduces the overlap between the π_g orbital and the Na^+ ion, hence causing the hyperfine coupling to be as small as $A_{III} = 0.07(1)\ \mathrm{T}/\mu_B$ in phase III. This is in sharp contrast to the case of CsO_2, where the lobe of π_g is directed to Cs^+, resulting in the large hyperfine coupling constant -1.16 T [9].

The power-law behavior of $1/T_1$ just above T_{S3} is indicative of a Tomonaga-Luttinger liquid (TLL) with a Luttinger parameter of $K = 0.25$, deduced from the relation $1/T_1 \propto T^{1/2K-1}$, where the transverse component of spin fluctuation dominates $1/T_1$ [31–34]. Note that the effect of the longitudinal component in spin fluctuation should become visible at a still lower-temperature region, where, however, the opening of the gap hides its effect [35]. The value of $K = 0.25$ agrees with the theoretical value of the $S = 1/2$ XXZ chain in the low-field limit [3]. That is, according to Ref. [3], in an ideally isotropic system the Luttinger parameter is $K = 0.5$, and an even slight anisotropy causes it to drop to 0.25. The investigation of the field dependence of K is unfortunately inaccessible, because of the large exchange constant J and the saturation field [5]. The kink of $1/T_1$ at 45 K suggests the crossover to the paramagnetic state. This type of precipitous change in various quantities including NMR-$1/T_1$ at the crossover between TLL and the paramagnetic state is often reported for other 1D spin chains [18,36–38].

Next, we focus on the small hump in $1/T_1$ at 13–15 K. Although this seems to indicate the existence of magnetic instability, no anomaly is observed in the other physical quantities, irrespective of macroscopic or microscopic, χ, M, C,

μSR, and the inelastic neutron scattering experiments, except for NMR-T_1 and the linewidth. We consider that this hump is brought about by a slowdown of spin fluctuation in the impurity phase, stated above. The concentration of 1.5% for impurity spins, which corresponds to the mean distance of roughly 1.8 nm, may be too long to allow the occurrence of the thermodynamical phase transition within the impurity system. So, these impurity spins only yield a slowdown of fluctuations below 18 K, causing the $1/T_1$ hump by the Bloembergen-Purcell-Pound (BPP) mechanism and also the linewidth increase [39]. A similar slowdown was reported in the other one-dimensional antiferromagnet $(CH_3)_2CHNH_3Cu(Cl_xBr_{1-x})_3$ [40]. Considering the existence of slowdown in the spin fluctuation at the considerably high temperature of 18 K, they are not free spins; a weak interaction via singlet dimers is expected. The observed $1/T_1$ is a superposition of two contributions: one from the impurity and the other from the host matrix. The contribution from the impurity propagates to the surroundings through spin diffusion. We have tentatively estimated the spin diffusion constant as $D = a^2/T_2 \simeq 4 \times 10^{-11}$ (cm^2/s), where $a \simeq 0.4$ nm is the average lattice constant and $T_2 = 40$ μs is the typical transverse NMR relaxation time in this system. The spin diffusion length $L = \sqrt{DT_1} \simeq 64$ nm within the typical value $T_1 \simeq 1$ s at 18 K sufficiently exceeds the averaged impurity-impurity distance. Consequently, the effect of spin diffusion effectively smears out the difference in $1/T_1$ within the system. This picture is consistent with the observation that the T_1 recovery curves consist of a single component in the entire temperature range including the hump.

Finally, we compare the present case with the prototypical spin-Peierls system $CuGeO_3$. In the latter, the spin-Peierls transition is drastically suppressed by a small concentration of impurity and the long-range magnetic order emerges when the impurity concentration exceeds the critical value. In NMR spectra, extra distinct peaks induced by impurities appear [41–43]. The present case qualitatively differs from $CuGeO_3$ in that the spin-Peierls transition is robust against the impurity effect.

ACKNOWLEDGMENT

This work was supported by JSPS KAKENHI under Grants No. 24K08364, No. 25H01546, and No. 25K07210.

DATA AVAILABILITY

The data that support the findings of this article are available upon reasonable request from the authors.

[1] Y. Zhou, K. Kanoda, and T.-K. Ng, Quantum spin liquid states, Rev. Mod. Phys. **89**, 025003 (2017).

[2] A. Vasiliev, O. Volkova, E. Zvereva, and M. Markina, Milestones of low-D quantum magnetism, npj Quantum Mater. **3**, 18 (2018).

[3] T. Giamarchi, *Quantum Physics in One Dimension* (Oxford University Press, Oxford, UK, 2003).

[4] M. Horvatić and C. Berthier, NMR studies of low-dimensional quantum antiferromagnets, in *High Magnetic Fields: Applications in Condensed Matter Physics and Spectroscopy*, edited by C. Berthier, L. P. Lévy, and G. Martinez (Springer, Berlin, 2001), pp. 191–210.

[5] M. Miyajima, F. Astuti, T. Fukuda, M. Kodani, S. Iida, S. Asai, A. Matsuo, T. Masuda, K. Kindo, T. Hasegawa, T. C. Kobayashi, T. Nakano, I. Watanabe, and T. Kambe, Spin-gap formation due to spin-Peierls instability in π-orbital-ordered NaO_2, Phys. Rev. B **104**, L140402 (2021).

[6] H. G. Smith, R. M. Nicklow, L. J. Raubenheimer, and M. K. Wilkinson, Antiferromagnetism in potassium superoxide KO_2, J. Appl. Phys. **37**, 1047 (1966).

[7] M. A. Bösch, M. E. Lines, and M. Labhart, Magnetoelastic interactions in ionic π-electron systems: Magnetogyration, Phys. Rev. Lett. **45**, 140 (1980).

[8] F. Astuti, M. Miyajima, T. Fukuda, M. Kodani, T. Nakano, T. Kambe, and I. Watanabe, Anionogenic magnetism combined with lattice symmetry in alkali-metal superoxide RbO_2, J. Phys. Soc. Jpn. **88**, 043701 (2019).

[9] M. Klanjšek, D. Arčon, A. Sans, P. Adler, M. Jansen, and C. Felser, Phonon-modulated magnetic interactions and spin Tomonaga-Luttinger liquid in the *p*-orbital antiferromagnet CsO_2, Phys. Rev. Lett. **115**, 057205 (2015).

[10] R. A. Ewings, M. Reehuis, F. Orlandi, P. Manuel, D. D. Khalyavin, A. S. Gibbs, A. D. Fortes, A. Hoser, A. J. Princep, and M. Jansen, Crystal and magnetic structure of cesium superoxide, Phys. Rev. B **108**, 174412 (2023).

[11] M. Miyajima, F. Astuti, T. Kakuto, A. Matsuo, D. P. Sari, R. Asih, K. Okunishi, T. Nakano, Y. Nozue, K. Kindo, I. Watanabe, and T. Kambe, Magnetism and high-magnetic field magnetization in alkali superoxide CsO_2, J. Phys. Soc. Jpn. **87**, 063704 (2018).

[12] K. Shibata, M. Naka, H. O. Jeschke, and J. Otsuki, Spin-orbital ordering in alkali superoxides, Phys. Rev. B **109**, 235115 (2024).

[13] M. Hase, I. Terasaki, and K. Uchinokura, Observation of the spin-Peierls transition in linear Cu^{2+} (spin-1/2) chains in an inorganic compound $CuGeO_3$, Phys. Rev. Lett. **70**, 3651 (1993).

[14] K. Uchinokura, Spin-Peierls transition in $CuGeO_3$ and impurity-induced ordered phases in low-dimensional spin-gap systems, J. Phys.: Condens. Matter **14**, R195 (2002).

[15] M. Itoh, S. Hirashima, and K. Motoya, ^{63,65}Cu NMR and NQR study of the Cu^{2+} electronic state and the spin dynamics in the spin-Peierls compound $CuGeO_3$, Phys. Rev. B **52**, 3410 (1995).

[16] M. Watanabe, N. Kurita, H. Tanaka, W. Ueno, K. Matsui, T. Goto, and M. Hagihala, Contrasting magnetic structures in $SrLaCuSbO_6$ and $SrLaCuNbO_6$: Spin-$\frac{1}{2}$ quasi-square-lattice J_1-J_2 Heisenberg antiferromagnets, Phys. Rev. B **105**, 054414 (2022).

[17] T. Goto, M. Fujihala, and S. Mitsuda, Correction to: ^{27}Al-NMR study on a square-kagome lattice antiferromagnet, Interactions **245**, 52 (2024).

[18] K. Matsui, A. Yagi, Y. Hoshino, S. Atarashi, M. Hase, T. Sasaki, and T. Goto, Rb-NMR study of the quasi-one-dimensional competing spin-chain compound $Rb_2Cu_2MO_3o_{12}$, Phys. Rev. B **96**, 220402(R) (2017).

[19] Y. Tanaka, M. Yoshida, M. Takigawa, Y. Okamoto, and Z. Hiroi, Novel phase transitions in the breathing pyrochlore lattice:

^{7}Li-NMR on $LiInCr_4O_8$ and $LiGaCr_4O_8$, Phys. Rev. Lett. **113**, 227204 (2014).

[20] K. Morioka, T. Goto, M. Watanabe, Y. Kojima, N. Kurita, H. Tanaka, S. Iguchi, and T. Sasaki, NMR study on equilateral triangular lattice antiferromagnet $Ba_2La_2CoTe_2O_{12}$, J. Low Temp. Phys. **222**, 47 (2026).

[21] A. Narath, Nuclear spin-lattice relaxation in hexagonal transition metals: Titanium, Phys. Rev. **162**, 320 (1967).

[22] K. Hashi, A. Oyamada, S. Maegawa, T. Goto, D. Li, and T. Suzuki, NMR study of a heavy fermion compound YbAs, J. Phys. Soc. Jpn. **67**, 4260 (1998).

[23] V. Epp, Ö. Gün, H.-J. Deiseroth, and M. Wilkening, Long-range Li^+ dynamics in the lithium argyrodite Li_7PSe_6 as probed by rotating-frame spin-lattice relaxation NMR, Phys. Chem. Chem. Phys. **15**, 7123 (2013).

[24] M. Horvatić, C. Berthier, Y. Fagot-Revurat, N. Piegay, M. Hanson, G. Dhalenne, and A. Revcolevschi, NMR study of the high magnetic field incommensurate phase of the $CuGeO_3$ spin-Peierls system, Physica B **246-247**, 22 (1998).

[25] N. Ishimura and H. Shiba, Effect of the magnetic field on the des Cloizeaux-Pearson spin-wave spectrum, Prog. Theor. Phys. **57**, 1862 (1977).

[26] M. Sato, T. Momoi, and A. Furusaki, NMR relaxation rate and dynamical structure factors in nematic and multipolar liquids of frustrated spin chains under magnetic fields, Phys. Rev. B **79**, 060406(R) (2009).

[27] N. Büttgen, K. Nawa, T. Fujita, M. Hagiwara, P. Kuhns, A. Prokofiev, A. P. Reyes, L. E. Svistov, K. Yoshimura, and M. Takigawa, Search for a spin-nematic phase in the quasi-one-dimensional frustrated magnet $LiCuVO_4$, Phys. Rev. B **90**, 134401 (2014).

[28] B. Kurniawan, H. Tanaka, K. Takatsu, W. Shiramura, T. Fukuda, H. Nojiri, and M. Motokawa, ESR study of the opening and closing of the field-induced gap in NH_4CuCl_3, Phys. Rev. Lett. **82**, 1281 (1999).

[29] H. Nojiri, H. Ohta, S. Okubo, O. Fujita, J. Akimitsu, and M. Motokawa, Submillimeter wave ESR study of spin gap excitations in $CuGeO_3$, J. Phys. Soc. Jpn. **68**, 3417 (1999).

[30] O. Fujita, J. Akimitsu, M. Nishi, and K. Kakurai, Evidence for a singlet-triplet transition in spin-Peierls system $CuGeO_3$, Phys. Rev. Lett. **74**, 1677 (1995).

[31] T. Suzuki and S.-I. Suga, NMR relaxation of quantum spin chains in magnetic fields, Phys. Rev. B **74**, 172410 (2006).

[32] S. Kobori, K. Matsui, H. Kuwahara, T. Goto, X. Zhang, Y. Nakano, S. Nishihara, K. Inoue, and T. Sasaki, Hyperfine Interact. **237**, 116 (2016).

[33] M. Jeong, H. Mayaffre, C. Berthier, D. Schmidiger, A. Zheludev, and M. Horvatić, Attractive Tomonaga-Luttinger liquid in a quantum spin ladder, Phys. Rev. Lett. **111**, 106404 (2013).

[34] M. Klanjšek, H. Mayaffre, C. Berthier, M. Horvatić, B. Chiari, O. Piovesana, P. Bouillot, C. Kollath, E. Orignac, R. Citro, and T. Giamarchi, Controlling Luttinger liquid physics in spin ladders under a magnetic field, Phys. Rev. Lett. **101**, 137207 (2008).

[35] T. Goto, T. Ishikawa, Y. Shimaoka, and Y. Fujii, Quantum spin dynamics studied by the nuclear magnetic relaxation of protons in the Haldane-gap system $(CH_3)_4NNi(NO_2)_3$, Phys. Rev. B **73**, 214406 (2006).

[36] Z. Honda, H. Aruga Katori, M. Ikeda, M. Hagiwara, K. Okunishi, M. Sakai, T. Fukuda, and N. Kamata, Magnetic field-induced phase transitions in the $S = 1/2$ two-leg spin-ladder material $Cu(DEP)Br_2$, J. Phys. Soc. Jpn. **81**, 113710 (2012).

[37] C. Rüegg, K. Kiefer, B. Thielemann, D. F. McMorrow, V. Zapf, B. Normand, M. B. Zvonarev, P. Bouillot, C. Kollath, T. Giamarchi, S. Capponi, D. Poilblanc, D. Biner, and K. W. Krämer, Thermodynamics of the spin Luttinger liquid in a model ladder material, Phys. Rev. Lett. **101**, 247202 (2008).

[38] B. Willenberg, H. Ryll, K. Kiefer, D. A. Tennant, F. Groitl, K. Rolfs, P. Manuel, D. Khalyavin, K. C. Rule, A. U. B. Wolter, and S. Süllow, Luttinger liquid behavior in the alternating spin-chain system copper nitrate, Phys. Rev. B **91**, 060407(R) (2015).

[39] N. Bloembergen, E. M. Purcell, and R. V. Pound, Relaxation effects in nuclear magnetic resonance absorption, Phys. Rev. **73**, 679 (1948).

[40] A. Oosawa, T. Suzuki, K. Kanada, S. Kojima, T. Goto, and H. Manaka, ^{1}H-NMR spin-lattice relaxation rate of the quantum spin system $(CH_3)_2CHNH_3Cu(Cl_xBr_{1-x})_3$ with $x = 0$ and 0.35, J. Phys. Soc. Jpn. **78**, 053702 (2009).

[41] M. Hase, Y. Sasago, I. Terasaki, K. Uchinokura, G. Kido, and T. Hamamoto, Effect of impurity on magnetic phase of spin-Peierls system; magnetization of $Cu_{1-x}Zn_xGeO_3$, J. Phys. Soc. Jpn. **65**, 273 (1996).

[42] J. Kikuchi, S. Ishiguro, T. Matsuoka, K. Motoya, T. Yamauchi, and Y. Ueda, Cu NMR and NQR studies of the doped spin-Peierls system $CuGe_{1-x}Si_xO_3$, Prog. Theor. Phys. Suppl. **145**, 345 (2002).

[43] M. Itoh, R. Tanaka, T. Yamauchi, and Y. Ueda, Cu NQR and NMR studies of impurity-doped spin-Peierls compounds $Cu_{1-x}Zn_xGeO_3$, Physica B **281-282**, 671 (2000).